Accepted Manuscript

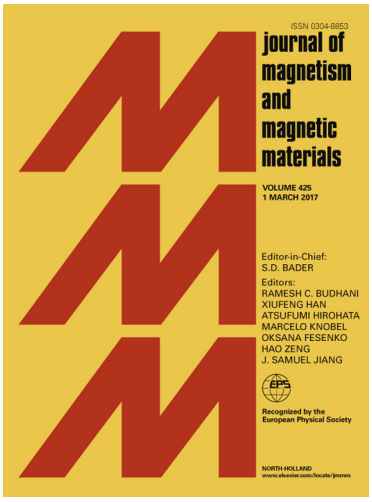

Mechanical manipulation of magnetic nanoparticles by magnetic force microscopy.

Jinyun Liu, Wenxiao Zhang, Yiquan Li, Hanxing Zhu, Renxi Qiu, Zhengxun Song, Zuobin Wang, Dayou Li

PII: S0304-8853(16)33337-6
DOI: http://dx.doi.org/10.1016/j.jmmm.2017.07.069
Reference: MAGMA 63000

To appear in: *Journal of Magnetism and Magnetic Materials*

Received Date: 12 December 2016
Revised Date: 26 May 2017
Accepted Date: 20 July 2017

Please cite this article as: J. Liu, W. Zhang, Y. Li, H. Zhu, R. Qiu, Z. Song, Z. Wang, D. Li, Mechanical manipulation of magnetic nanoparticles by magnetic force microscopy., *Journal of Magnetism and Magnetic Materials* (2017), doi: http://dx.doi.org/10.1016/j.jmmm.2017.07.069

Title：

Mechanical manipulation of magnetic nanoparticles by magnetic force microscopy.

Author

Jinyun Liu[a,b], Wenxiao Zhang[a], Yiquan Li[c], Hanxing Zhu[d], Renxi Qiu[b], Zhengxun Song[a], Zuobin Wang[a,b,*], Dayou Li[b,*].

Affiliations:

[a]International Research Centre for Nano Handling and Manufacturing of China, Changchun University of Science and Technology, Changchun 130022, China;

[b]Institute for Research in Applicable Computing, University of Bedfordshire, Luton LU1 3JU, UK;

[c]College of Mechanical and Electric Engineering, Changchun University of Science and Technology, Changchun 130022, China;

[d]School of Engineering, Cardiff University, Cardiff CF24 3AA, UK

Corresponding authors:

Zuobin Wang: phone: +86 431 85582341; fax number: +86 431 85582925; email address: wangz@cust.edu.cn

Dayou Li: phone: +44 1582 489371; fax number: +44 1582 489212; email address: dayou.li@beds.ac.uk

Abstract

A method has been developed in this work for the mechanical manipulation of magnetic nanoparticles (MNPs). A helical curve was designed as the capture path to pick up and remove the target nanoparticle on a mica surface by a magnetic probe based on the magnetic force microscope (MFM). There were magnetic, tangential and pushing forces acting on the target particle during the approaching process when the tip followed the helical curve as the capture path. The magnetic force was significant when the tip was closer to the particle. The target particle can be attached on the surface of the magnetic probe tip and then be picked up after the tip retracted from the mica surface. Theoretical analysis and experimental results were presented for the pick-up and removal of MNPs. With this method, the precision and flexibility of manipulation of MNPs were improved significantly compared to the pushing or sliding of the target object away from the corresponding original location following a planned path.

Keywords: Magnetic nanoparticles; Magnetic force microscope; Mechanical manipulation; Capture path

1. Introduction

Manipulation of atoms, molecules and nano materials has been applied to many scientific and technological areas, such as biology, medicine, physics and chemistry [1-4]. Due to the high resolution of atomic force microscope (AFM), it is a proper tool for the imaging and manipulation of nano objects [5, 6]. Korayem and Saraee et al. [7-9] modeled and simulated the pushing and sliding of nanoparticles by AFM for

biological sample separation and positioning. Hsieh et al. [10] utilized the AFM tip to push the gold nanorods, demonstrating that it can be used for the building of blocks in nano-fabrication. Requicha et al. [3] pushed Au nanoparticles of 15 nm in diameter upon a mica surface to form an array by AFM tip.

Based on the AFM, the magnetic force microscope (MFM) is developed for the study of magnetic domain structures on a submicron/nanometer scale [11]. Besides the observation of magnetic structures, MFM is commonly used for the manipulation and measurement of magnetic samples with the magnetic probe [12]. Due to the unique features of magnetic nanoparticles (MNPs), such as the high reactivity, high surface area and biocompatibility [13], MNPs are widely used for the targeting of specific diseases, drug delivery, magnetic resonance imaging [14], electronic device [15] and sewage disposal [16]. In addition, MFM has been used for the manipulation of MNPs. Chang et al. [17] reversed the magnetization of magnetic nanoparticles with the inhomogeneous magnetic field produced by the magnetic tip. Baronov and Andersson [18] tracked a magnetic nanoparticle by MFM and a tracking control law was developed for the magnetic tip retained adjacent to the target magnetic particle. Pinilla-Cienfuegos et al. [19] manipulated individual molecules based on magnetic nanoparticles with an average size of 25 nm by MFM. The pushing or sliding of a target object along a planned straight line path is currently the main method in manipulations. However, the target object is manipulated laterally and hard to be removed away from the surface with those methods. If the reposition precision of the manipulation system is low, the tip will be hard to precisely follow the designed path and push or slide the target nanoparticle. The flexibility of the manipulations is limited due to the planned path being a straight line in many applications [15].

In this work, a method proposed for the mechanical manipulation of MNPs. A

helical curve was designed as the capture path to precisely manipulate the MNPs. Theoretical analysis and experimental results have shown that MNPs can be manipulated successfully by this method. The details are described in the following sections.

2. Materials and methods

2.1 Sample preparation

Fe_3O_4 magnetic nanoparticles were synthesized by the co-precipitation method [20] and the MNPs were functioned by acetate for the dispersion. 2.5 μg/mL of MNPs were dispersed by ultrasounds for 30 minutes below 30℃. 2.5 μL of the solution was deposited on the surface of mica and dried at room temperature in the air. The diameters of MNPs were in the range of 10 nm to 100 nm.

2.2 MFM system

A JPK (NanoWizard®3, Germany) MFM system was used for the imaging and manipulation of MNPs carried out in the air condition. The MFM used in the experiment was equipped with a closed loop scanner. The typical spring constant of the utilized magnetic probe was 3 N/m and the resonant frequency was 75 kHz (MagneticMulti75-G, BudgetSensors). The tip was magnetized by an external magnet field in the vertical direction.

Two successive scans with a lift-tapping mode were used for MFM imaging. In the first scan, the topography image was obtained with a tapping mode. In the second scan, the probe was lifted several nanometers from the surface and traced the topography profile to obtain the magnetic force map. A manipulation mode (contact)

was used for drawing the capture path on the substrate surface and picking up the target magnetic nanoparticle. To successful pick up the target nanoparticle, the helical curve was drawn from the outer to inside and the ending position was located on the target nanoparticle, and the curve with at least 3 turns.

3. Theory

The diameter of particle size being less than 100 nm, leads to the particle superparamagnetic or paramagnetic character [21]. The significant feature of superparamagnetic particles is that they will only be magnetized by an applied magnetic field, consequently presenting a single magnetic domain with a moment of the magnetic direction being impacted by the applied magnetic field [22, 23]. The MNPs magnetized by a magnetic probe are shown in Fig. 1. Additionally, the single magnetic domain direction of MNPs is presented.

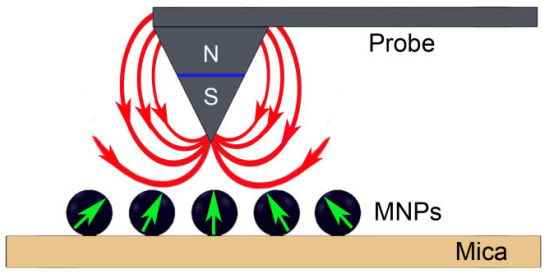

Fig. 1. Magnetic domain directions of MNPs magnetized by magnetic probe.

(1-column, dpi:600, size: 8.00cm×4.00cm)

A helical curve was designed as the capture path and it was followed by the magnetic tip for manipulating the MNPs, as shown in Fig. 2(a). The lift-tapping mode was first used for scanning the distributions of MNPs on the mica surface and a nanoparticle was selected as the target to be picked up. It was then switched to the

manipulation mode drawn a helical curve, and moved the tip along the designed helical path with a specified speed and pushing force to approach the target nanoparticle, as presented in Fig. 2(b). The force for the scanning was smaller than that for operating the nanoparticle. Finally, the tip was retracted from the mica surface and the nanoparticle was picked up, as shown in Fig. 2(c).

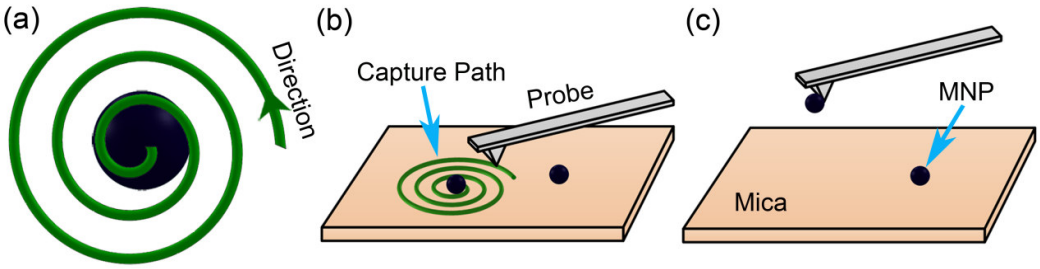

Fig. 2. Mechanical manipulation of MNPs. (a) A helical curve was designed as the capture path. (b) The probe followed the capture path to approach the target MNP. (c) The target MNP was picked up by magnetic tip and removed from the mica surface. (2-column, dpi:600, size: 17.00cm×4.50cm)

The interaction forces between the magnetic probe and the MNP in the approaching process are presented in Fig. 3. Fig. 3(a) shows the forces acting on the MNP during the process of tip approaching to the target nanoparticle on the mica surface in the x/y plane. F_m is the magnetic force to attract the nanoparticle attached to the tip surface. F_r is the resistance force against the particle to move, whereas it constitutes with the van der Waals', capillary, electrostatic and friction forces between the particle and the substrate surface. In the approaching process, there should be a maximum value for F_r. When F_m is not large enough, the nanoparticle does not move on the surface, namely at the equilibrium state, thus $F_m=F_r$. Apparently, the magnetic force direction always changes when the tip move along the capture path and the

value of F_m increases with the decrease of the distance between the probe and the particle. The F_m acting onto the particle is presented in Fig. 3(b).

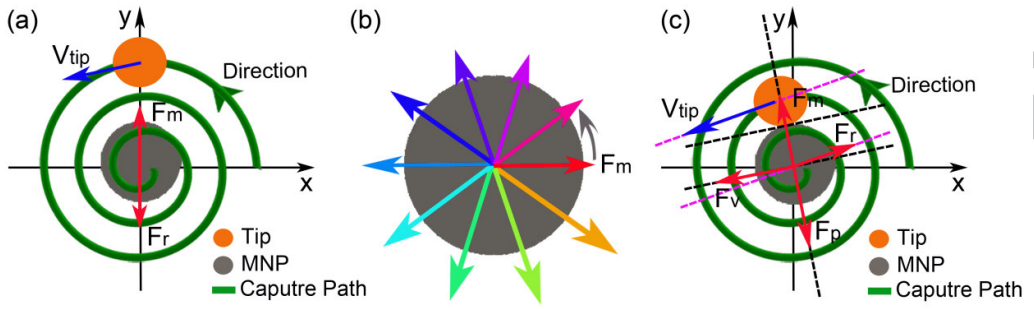

Fig. 3. Forces acting on the MNP on the substrate surface in the process of tip approaching. (a) Forces acting on the particle when the magnetic tip approaching to the particle. (b) Magnetic force alteration when the magnetic tip approaching to the particle. (c) Forces acting on the MNP when the magnetic tip contacts the particle. (2-column, dpi:600, size: 17.00cm×5.00cm)

As shown in Fig. 3(c), the magnetic force F_m will reach its maximum value with the direction towards the tip when the magnetic tip contacts the target particle. The tangential force F_v is parallel to the tangential direction of the tip and the particle contact surface. The push force F_p is opposite to the direction of F_m, and F_p is proven to be controllable and set by the MFM system. F_r is opposite to the tangential direction of the moving path against the particle moving on the surface. The directions of F_m, F_v, F_p and F_r are always changed during the movements of the tip following the designed helical path. Due to the existence of F_v and F_p, when the tip moves along the capture path and pushes the particle, the particle will be slid on the substrate and then F_r will be decreased to the minimum [24-26].

The tip will retract from the mica surface when the MNP is attached on the tip

surface, as shown in Fig. 2(c). The force model of the magnetic tip picking up the MNP vertically is presented in Fig. 4 [27-29].

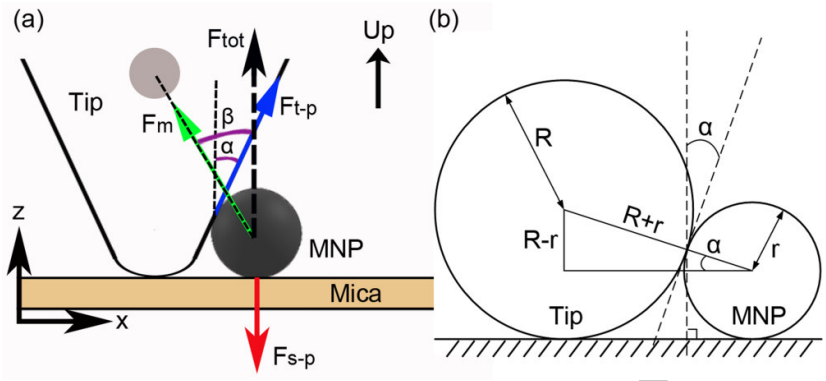

Fig. 4. Force model of magnetic tip picking up the MNP vertically. (a) Forces during the pick-up of the particle by the magnetic tip. (b) Angle between the tip and the particle. (2-column, dpi:600, size: 11.60cm×5.30cm)

In Fig. 4(a), the forces are expressed as [30]

$$F_{t-p} = F_{tv} + F_{tc} + F_{te} + f_{t-p} \tag{1}$$

$$F_{s-p} = F_{sv} + F_{sc} + F_{se} + F_g + f_{s-p} \tag{2}$$

where $F_{t\text{-}p}$ and $F_{s\text{-}p}$ are the tip-particle and surface-particle forces, respectively, including the van der Waals' force F_{tv} and F_{sv} [31], capillary force F_{tc} and F_{sc} [32, 33], electrostatic force F_{te} and F_{se} [34]. $f_{t\text{-}p}$ is the friction force between the tip surface and the particle, $f_{s\text{-}p}$ is the adhesion force between the substrate surface and the particle [27, 35], and F_g is the gravity of the particle.

F_m is the magnetic force between the tip and the particle [18]. F_{tot} is the total interaction force of $F_{t\text{-}p}$ and F_m in the vertical direction. It can be expressed as

$$F_{\text{tot}} = F_{t-p}\cos\alpha + F_m\cos\beta \tag{3}$$

Because the tip radius R is smaller than 60 nm and the radius of nanoparticle r is smaller than 50 nm, the value of $\cos\alpha$ is close to 1. The tip height is 17 μm and

significantly larger than the particle size. The angle β is very small and it can be assumed to be 0. Thus, Eq. (3) can be calculated by

$$F_{\text{tot}} \approx F_{t-p} + F_m \tag{4}$$

The vertical direction force of the particle is:

$$F_p\big|_z = F_{tot} - F_{s-p} \tag{5}$$

Since the van der Waals', capillary, electrostatic forces and friction exist simultaneously at the tip and the mica surface, it can be assumed that $F_{tv}=F_{sv}$, $F_{tc}=F_{sc}$, $F_{te}=F_{se}$ and $f_{t\text{-}p}=f_{s\text{-}p}$. Combining Eqs. (1), (2) and (4), Eq. (5) can be rewritten as

$$F_p\big|_z \approx F_m - F_g \tag{6}$$

Due to the small particle gravity of the particles used ranging from 10 nm to 100 nm in diameter [36], and the superparamagnetic character of nanoparticles, F_m will be large enough if the particle is attached on the tip surface and the following relation is observed: $F_m >> F_g$. Thus, the particle can be separated from the mica surface and picked up by the magnetic tip.

4. Results and Discussion

In the experiment, the MNPs with a diameter of 30 nm were manipulated by the proposed method. The results were presented in Fig. 5. The target particle was selected and labeled by a circle, as shown in Fig. 5(a), whereas the corresponding magnetic domain distribution was presented in Fig. 5(b). The capture path used for the target particle manipulation was drawn as a green helical curve, as presented in Fig. 5(c). The magnetic tip followed the designed helical path approaching to the target particle and finally the particle was attached onto the tip surface. The particle was removed from the mica surface after the tip retracted, as presented in Fig. 5(d) and the corresponding magnetic domain of the particle did not exist, as shown in Fig.

5(e). The lift height was 7 nm for MFM imaging. The speed for the capture of the particle was 0.3 μm/s and the applied force was 45 nN.

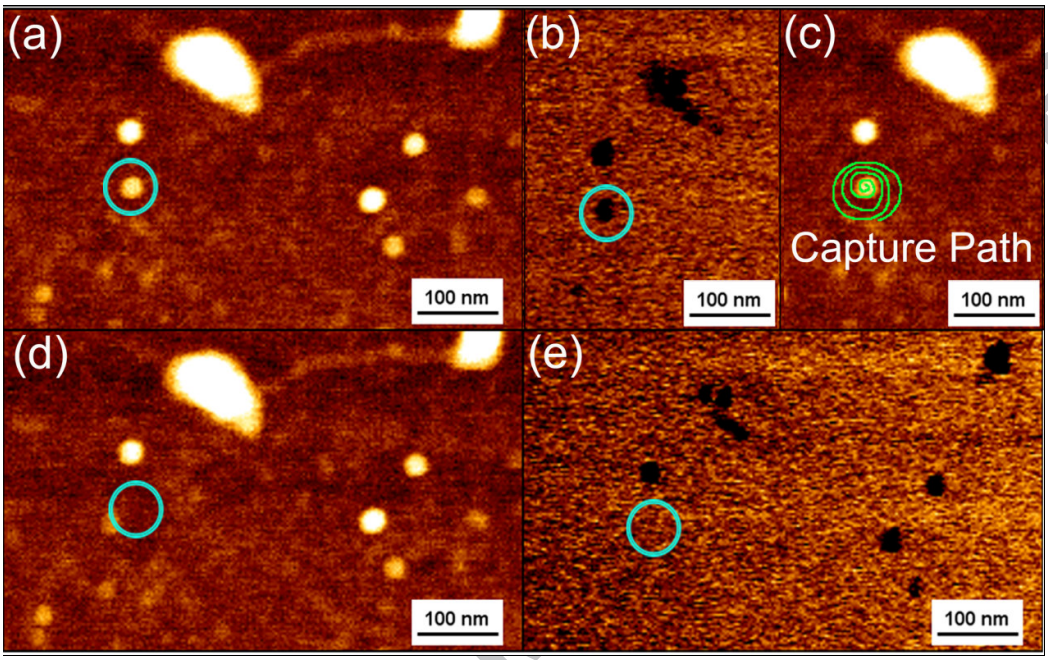

Fig. 5. Images of MNPs previous to and following the manipulation by MFM. (a) The topography image of MNPs before the pick-up. (b) The corresponding MFM image of (a). (c) Shows the helical curve designed as the capture path for the particle pick-up. (d) The topography image of the target particle after the pick-up. (e) The corresponding MFM image of (d). (2-column, dpi:300, size: 17.00cm×10.60cm)

For the evaluation of the method in terms of flexibility and control capability, a series of manipulations were successively carried out for three targeted MNPs. The results were presented in Fig. 6. It can be clearly observed that particle P1 with a diameter of 25 nm, particle P2 with a diameter of 15 nm and particle P3 with a diameter of 40 nm were successively picked up. In the experiment, the lift height was 7 nm for MFM imaging. The capture speed of particles was 0.3 μm/s and the push

force was 60 nN.

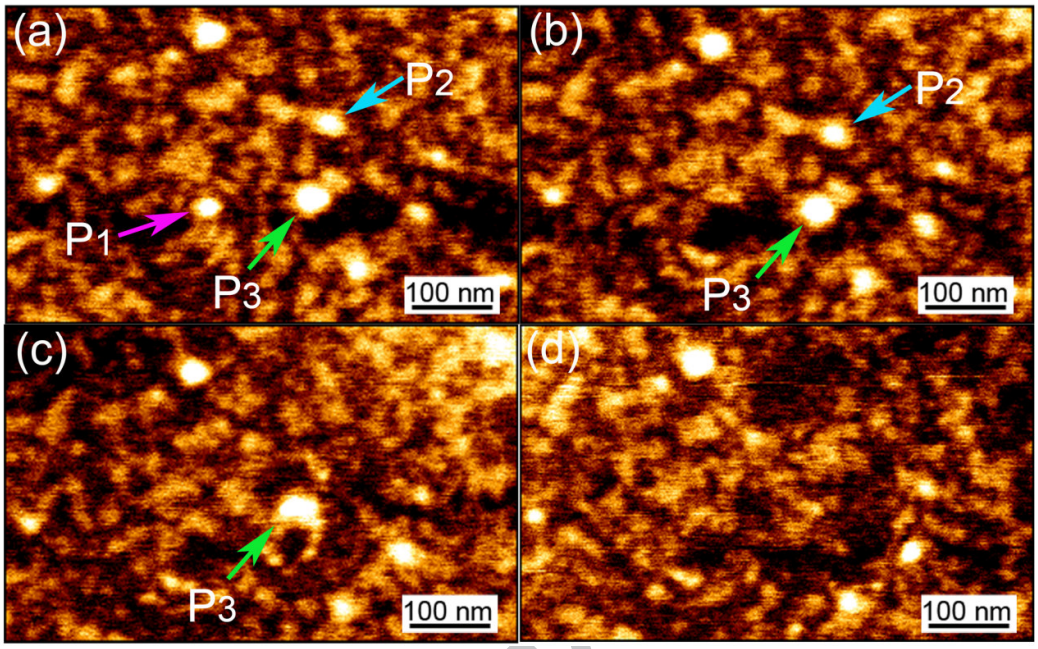

Fig. 6. Successive manipulations of three MNPs. (a) The topography image of MNPs previous to the pick-up, particles P1, P2 and P3 displayed with arrows. (b) The result following the pick-up of particle P1. (c) The removal result of particle P2. (d) The following pick-up result of particle P3. The arrows were corresponding to the target particles. (2-column, dpi:300, size: 17.00cm×10.50cm)

Xu et al. [37] used a hybrid-conductive AFM probe to manipulate Au nanoparticles. Mirowski et al. [38] provided the magnetic field gradient by magnetic probe to sort out magnetic particles on an microfluidic platform with an array of magnetic trap elements and the particle size was 1 μm in diameter. Currently, the common methods used for the manipulation of single nanoscale objects by AFM are pushing, rolling, cutting, drilling and dissecting [7-9]. Also, the main methods are pushing and sliding of the particle along a linear path. With the methods, the target

particle can be moved from one position to another position on the surface [9, 27, 28]. For the particles with disordered and complicated distributions, it is hard to design a simple straight line path for the tip to push a selected particle to the target location. In practice, the linear path should be precisely determined for each operation, and it is difficult to be successfully performed. Due to the limitation of the tip radius, reliability and reposition precision of the AFM system, flexible manipulation of particles with a size below 100 nm is still a challenge [27].

Because the interaction forces between the substrate surface and the particle are difficult to overcome in the vertical direction, it is hard to separate the particle away from the surface and pick up it by the method of simple tip approaching and retracting.

For the proposed helical path method, the pushing force and tangential force in the horizontal direction make the particle moving on the surface when the tip contacts the particle. Due to the role of tangential force, the particle will be rotated under the moment and the contact area between the particle and the surface will be decreased. Accordingly, the forces between the particle and the substrate surface are reduced. When the particle attached onto the tip surface and the tip is retracted from the surface, it can be picked up with the attractive magnetic force. The MNPs can also be removed from the tip using an external magnetic field and a BOPP film [39].

In the experiments, MNPs were successfully picked up and removed with the proposed method. The success rate of pick up the MNPs by the proposed method was >90 % for the MNPs with the diameters of 10~90 nm, and the success rate was ~50 % for the MNPs with the diameters of 100~200 nm.

5. Conclusions

In this work, MNPs were picked up and removed with the magnetic probe following a designed capture path, being the helical curve. It can be described that due to the interactions of tangential, pushing and magnetic forces caused by magnetic probe movements, the resistance force is reduced and the particle can be attached on the surface of the magnetic probe tip when the tip contacts the particle. The experimental results indicate that with this method MNPs can be picked up and removed successfully on the mica surface. The method significantly improves the precision and flexibility of manipulations, and provides a guide for the manipulation of MNPs for different applications.

Acknowledgments

This work was supported by EU FP7 (BioRA No.612641), China-EU H2020 (FabSurfWAR Nos. 2016YFE0112100 and 644971), EU H2020 (MNR4SCell No.734174), International Science and Technology Cooperation Program of China (No.2012DFA11070), and Jilin Provincial Science and Technology Program (Nos.20140414009GH, 20140622009JC and 20160623002TC).

Conflict of interest

The authors declare that they have no conflict of interest.

References

[1] S.G. Kaminskyj, T.E. Dahms, High spatial resolution surface imaging and analysis of fungal cells using SEM and AFM, Micron 39 (2008) 349-361.

[2] O. Guillermet, S. Gauthier, C. Joachim, P. Mendoza, T. Lauterbach, A. Echavarren, STM and AFM high resolution intramolecular imaging of a single decastarphene molecule, Chem. Phys. Lett. 511 (2011) 482-485.
[3] A.A.G. Requicha, D.J. Arbuckle, B. Mokaberi, J. Yun, Algorithms and software for nanomanipulation with atomic force microscopes, Int. J. Robot. Res. 28 (2009) 512-522.
[4] Z. Wang, D. Li, J. Zhang, Robotic nanoassembly current developments and challenges, Int. J. Comput. Appl. T. 41 (2011) 185-194.
[5] H.K. Graham, N.W. Hodson, J.A. Hoyland, S.J. Millward-Sadler, D. Garrod, A. Scothern, C.E. Griffiths, R.E. Watson, T.R. Cox, J.T. Erler, A.W. Trafford, M.J. Sherratt, Tissue section AFM: In situ ultrastructural imaging of native biomolecules, Matrix. Biol. 29 (2010) 254-260.
[6] P. Milhiet, F. Gubellini, A. Berquand, P. Dosset, J. Rigaud, C.L. Grimellec, D. Lévy, High-resolution AFM of membrane proteins directly incorporated at high density in planar lipid bilayer, Biophys. J. 91 (2006) 3268-3275.
[7] M.H. Korayem, M.B. Saraee, Z. Mahmoodi, S. Dehghani, Modeling and simulation of three dimensional manipulations of biological micro/nanoparticles by applying cylindrical contact mechanics models by means of AFM, J. Nanopart. Res. 17 (2015) 439.
[8] M.B. Saraee, M.H. Korayem, Dynamic simulation and modeling of the motion modes produced during the 3D controlled manipulation of biological micro/nanoparticles based on the AFM, J. Theor. Biol. 378 (2015) 65-78.
[9] M.H. Korayem, M. Zakeri, Dynamic modeling of manipulation of micro/nanoparticles on rough surfaces, Appl. Surf. Sci. 257 (2011) 6503-6513.
[10] S. Hsieh, S. Meltzer, C.R. Chris Wang, A.A.G. Requicha, M.E. Thompson, B.E. Koel, Imaging and manipulation of gold nanorods with an atomic force microscope, J. Phys. Chem. B. 106 (2002) 231-234.
[11] V. Cambel, P. Elias, D. Gregusova, J. Martaus, J. Fedor, G. Karapetrov, V. Novosad, Magnetic elements for switching magnetization magnetic force microscopy tips, J. Magn. Magn. Mater. 322 (2010) 2715-2721.
[12] D. Passeri, C. Dong, L. Angeloni, F. Pantanella, T. Natalizi, F. Berlutti, C. Marianecci, F. Ciccarello, M. Rossi, Thickness measurement of soft thin films on periodically patterned magnetic substrates by phase difference magnetic force microscopy, Ultramicroscopy 136 (2014) 96-106.
[13] A. Akbarzadeh, M. Samiei, S. Davaran, Magnetic nanoparticles preparation, physical properties, and applications in biomedicine, Nanoscale Res. Lett. 7 (2012) 1-13.
[14] E.E.L. Lewis, H.W. Child, A. Hursthouse, D. Stirling, M. McCully, D. Paterson, M. Mullin, C.C. Berry, The influence of particle size and static magnetic fields on the uptake of magnetic nanoparticles into three dimensional cell-seeded collagen gel cultures, J. Biomed. Mater. Res. B. Appl. Biomater. 103 (2015) 1294-1301.
[15] A. Sarella, A. Torti, M. Donolato, M. Pancaldi, P. Vavassori, Two-dimensional programmable manipulation of magnetic nanoparticles on-chip, Adv. Mater. 26 (2014) 2384-2390.
[16] P. Xu, G.M. Zeng, D.L. Huang, C.L. Feng, S. Hu, M.H. Zhao, C. Lai, Z. Wei, C. Huang, G.X. Xie, L.Z. F., Use of iron oxide nanomaterials in wastewater treatment: A review, Sci. Total. Environ. 424 (2012) 1-10.
[17] J. Chang, H. Yi, H. Cheol Koo, V.L. Mironov, B.A. Gribkov, A.A. Fraerman, S.A. Gusev, S.N. Vdovichev, Magnetization reversal of ferromagnetic nanoparticles under inhomogeneous magnetic field, J. Magn. Magn. Mater. 309 (2007) 272-277.

[18] D. Baronov, S.B. Andersson, Tracking a magnetic nanoparticle in 3-D with a magnetic force microscope, In Proceedings of the 47th IEEE Conference on Decision and Control (CDC), Cancun, Mexico (2008) pp 5170-5175.
[19] E. Pinilla-Cienfuegos, S. Kumar, S. Mañas-Valero, J. Canet-Ferrer, L. Catala, T. Mallah, A. Forment-Aliaga, E. Coronado, Imaging the magnetic reversal of isolated and organized molecular-based nanoparticles using magnetic force microscopy, Part. Part. Syst. Char. 32 (2015) 693-700.
[20] Y.S. Kang, S. Risbud, J.F. Rabolt, P. Stroeve, Synthesis and characterization of nanometer-size Fe_3O_4 and γ-Fe_2O_3 particles, Chem. Mater. 8 (1996) 2209-2211.
[21] S. Schreiber, M. Savla, D.V. Pelekhov, D.F. Iscru, C. Selcu, P.C. Hammel, G. Agarwal, Magnetic force microscopy of superparamagnetic nanoparticles, Small 4 (2008) 270-278.
[22] T.M. Nocera, J. Chen, C.B. Murray, G. Agarwal, Magnetic anisotropy considerations in magnetic force microscopy studies of single superparamagnetic nanoparticles, Nanotechnology 23 (2012) 495704.
[23] S. Prijic, J. Scancar, R. Romih, M. Cemazar, V.B. Bregar, A. Znidarsic, G. Sersa, Increased cellular uptake of biocompatible superparamagnetic iron oxide nanoparticles into malignant cells by an external magnetic field, J. Membr. Biol. 236 (2010) 167-179.
[24] M. Palacio, B. Bhushan, A nanoscale friction investigation during the manipulation of nanoparticles in controlled environments, Nanotechnology 19 (2008) 315710.
[25] D. Guo, J. Li, L. Chang, J. Luo, Measurement of the friction between single polystyrene nanospheres and silicon surface using atomic force microscopy, Langmuir 29 (2013) 6920-6925.
[26] D. Maharaj, B. Bhushan, S. Iijima, Effect of carbon nanohorns on nanofriction and wear reduction in dry and liquid environments, J. Colloid. Interf. Sci. 400 (2013) 147-160.
[27] M. Sitti, H. Hashimoto, Controlled pushing of nanoparticles: modeling and experiments, In Proceedings of IEEE/ASME Transactions on Mechatronics, (2000) pp 199-211.
[28] M.H. Korayem, M. Zakeri, Sensitivity analysis of nanoparticles pushing critical conditions in 2-D controlled nanomanipulation based on AFM, Int. J. Adv. Manuf. Tech. 41 (2009) 714-726.
[29] D. Baronov, S.B. Andersson, Controlling a magnetic force microscope to track a magnetized nanosize particle, IEEE T. Nanotechnol. 9 (2010) 367-374.
[30] N.V. Zarate, A.J. Harrison, J.D. Litster, S.P. Beaudoin, Effect of relative humidity on onset of capillary forces for rough surfaces, J. Colloid. Interf. Sci. 411 (2013) 265-272.
[31] H.J. Butt, B. Cappella, M. Kappl, Force measurements with the atomic force microscope: Technique, interpretation and applications, Surf. Sci. Rep. 59 (2005) 1-152.
[32] E. Hsiao, M.J. Marino, S.H. Kim, Effects of gas adsorption isotherm and liquid contact angle on capillary force for sphere-on-flat and cone-on-flat geometries, J. Colloid. Interf. Sci. 352 (2010) 549-557.
[33] G. Lian, J. Seville, The capillary bridge between two spheres: New closed-form equations in a two century old problem, Adv. Colloid. Interfac. 227 (2016) 53-62.
[34] S. Belaidi, P. Girard, G. Leveque, Electrostatic forces acting on the tip in atomic force microscopy: Modelization and comparison with analytic expressions, J. Appl. Phys. 81 (1997) 1023-1030.

[35] G.V. Dedkov, Friction on the nanoscale: new physical mechanisms, Mater. Lett. 38 (1999) 360-366.
[36] S. Kayal, D. Bandyopadhyay, T.K. Mandal, R.V. Ramanujan, The flow of magnetic nanoparticles in magnetic drug targeting, RSC Adv. 1 (2011) 238-246.
[37] J. Xu, K.J. Kwak, J.L. Lee, G. Agarwal, Lifting and sorting of charged Au nanoparticles by electrostatic forces in atomic force microscopy, Small 6 (2010) 2105-2108.
[38] E. Mirowski, J. Moreland, A. Zhang, S.E. Russek, M.J. Donahue, Manipulation and sorting of magnetic particles by a magnetic force microscope on a microfluidic magnetic trap platform, Appl. Phys. Lett. 86 (2005) 243901.
[39] C. Zhang, J. Liu, Q. Meng, W. Zhang, Y. Wang, D. Li, Z. Wang, Cleaning of contaminated MFM probes using a BOPP film and external magnetic field, Micron 97 (2017) 1-5.

Highlights

1. The magnetic probe on an MFM was used to manipulate magnetic nanoparticles (MNPs).
2. A helical curve was designed as the capture path to pick up the target MNPs.
3. The target MNPs can be attached on the tip surface of the magnetic probe.
4. The manipulation precision and flexibility of MNPs were significantly improved.